Bulletin of the Seismological Society of America, Vol. 99, No. 6, pp. 3502–3509, December 2009, doi: 10.1785/0120090128

Short Note

Runup Distribution for the 1908 Messina Tsunami in Italy: Observed Data versus Expected Curves

by Andrea Billi,* Liliana Minelli,† Barbara Orecchio, and Debora Presti

Abstract The source of the catastrophic 1908 Messina tsunami, southern Italy, is studied by best-fitting the available datasets of observed runup with a previously published empirical function (i.e., the expected runup distribution). The maximum runup is ~12 m and was measured ~30–40 km to the south of the area where the maximum coseismic dislocation and Mercalli–Cancani–Sieberg (MCS) intensities were recorded. The observed runup drops from ~12 m to less than 1 m in a few tens of kilometers. The comparison between observed and expected runup distributions suggests that the main cause of the 1908 tsunami was a mass failure, thus supporting previously published evidence including tsunami arrival times, bathymetric maps, and chronicles reporting the interruption of submarine cables. This article adds a significant case history to the very limited database of thoroughly documented runup for landslide tsunamis.

Online Material: Tsunami runup data and histograms of statistical parameters.

Introduction

The collection of tsunami runup data and analysis of their spatial distribution are very important to understand the cause of the parent tsunami, to forecast plausible scenarios of future events, and to establish a reliable database, against which numerical and physical models should be tested for a proper validation (e.g., Borrero *et al.*, 2003; Davies *et al.*, 2003; Okal *et al.*, 2003; Borrero *et al.*, 2006; Synolakis and Kong, 2006; Ioualalen *et al.*, 2007; Tappin ,Watts, and Grilli, 2008; Borrero *et al.*, 2009; Synolakis and Kânoğlu, 2009). In particular, understanding the source of a tsunami when it is caused by a seismically triggered submarine landslide is usually very challenging because of the paucity of detectable evidence. In the case of the 1998 Papua New Guinea tsunami, for instance, the hydroacoustic record proved to be the defining factor in recognizing this event as a landslide tsunami (Synolakis *et al.*, 2002); when such evidence is lacking, however, the runup distribution is one of the most important clues to discriminate between possible tsunami sources (e.g., Okal and Synolakis, 2004; Fritz *et al.*, 2007; Gerardi *et al.*, 2008; López-Venegas *et al.*, 2008; Okal *et al.*, 2009).

Billi *et al.* (2008) addressed the problem of the source (i.e., seismic dislocation or mass failure) for the catastrophic 1908 Messina tsunami, Ionian Sea (Fig. 1), concluding that a submarine mass failure was the main source of the tsunami. This conclusion was based on a series of evidence including tsunami arrival times and bathymetric maps, as well as chronicles reporting the interruption of submarine cables (Baratta, 1910; Ryan and Heezen, 1965). Billi *et al.* (2008) also displayed the tsunami runup data, which, however, were not compared with the expected distribution of earthquake and landslide tsunami runup (e.g., Okal and Synolakis, 2004), thus leaving these data substantially unexplained. More recently, Gerardi *et al.* (2008), by analyzing a dataset of tsunami runup partially different from that shown by Billi *et al.* (2008), concluded that the 1908 tsunami was caused by the seismic dislocation.

In this article, we analyze the runup datasets available in the literature for the 1908 tsunami (Platania, 1909; Baratta, 1910; Gerardi *et al.*, 2008) and discriminate between the possible tsunami sources by best-fitting these datasets with the function of expected tsunami runup proposed by Okal and Synolakis (2004) as described next.

Our study includes some important implications. The first implication concerns the tsunami hazard in the Ionian Sea. Knowing the causes and effects of past tsunamis is, in fact, fundamental to estimate the potential risk in this region.

The second implication concerns modeling of the causative fault for the 1908 Messina earthquake ($M \approx 7.1$), which was one of the most destructive ever documented in the Mediterranean area (Boschi *et al.*, 2000). This causative fault

*Now at CNR-IGAG, Istituto di Geologia Ambientale e Geoingegneria, Rome, Italy.

†Now at Dipartimento di Scienze della Terra, Università di Roma "La Sapienza", Rome, Italy.

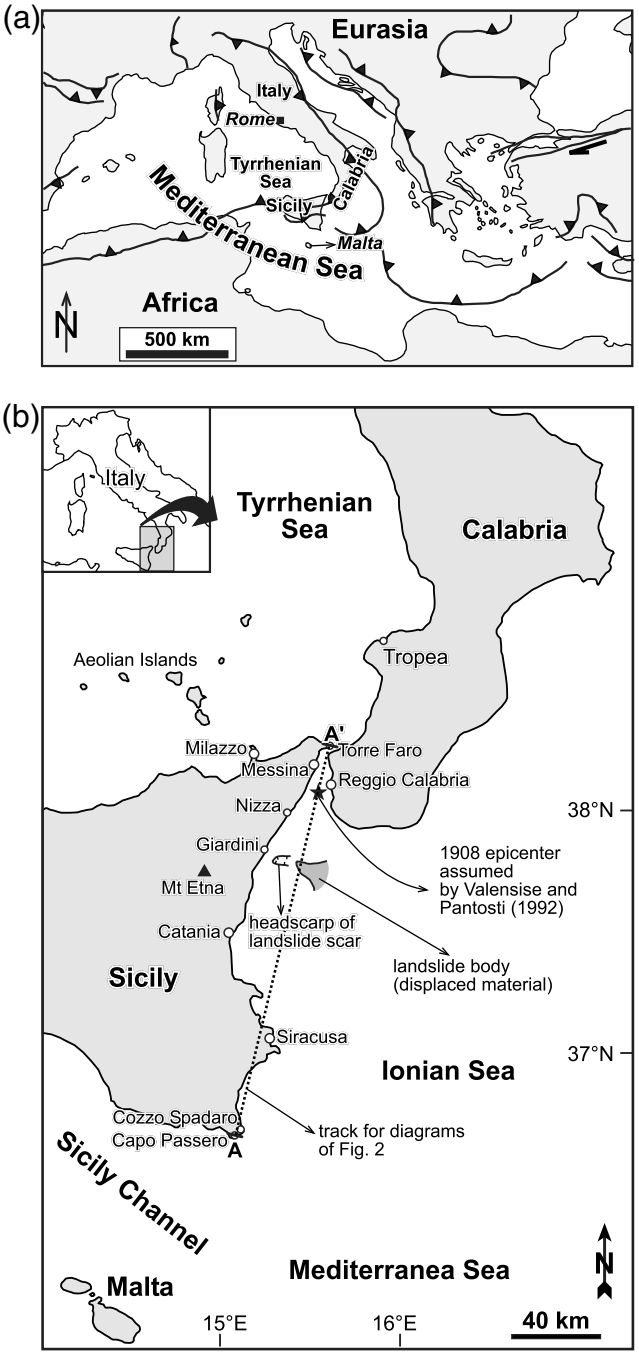

Figure 1. (a) Schematic tectonic setting of the central Mediterranean area. Main orogenic belts along the convergent Africa–Eurasia plate boundary are shown. (b) Map of the Messina Straits area, southern Italy, and surrounding areas. The underwater landslide drawn off Giardini, Ionian Sea, has been proposed as the likely cause for the 1908 Messina tsunami (Billi *et al.*, 2008).

is substantially still unknown (Pino *et al.*, 2009). One important element of confusion is whether the related tsunami was caused by the seismic dislocation or not and, therefore, whether the tsunami data (e.g., runup and arrival times) should be considered or not in identifying and modeling the fault (e.g., Tinti and Armigliato, 2003).

The third implication concerns the tsunami science in general. The database of thoroughly documented runup for landslide tsunamis is very limited. For instance, Okal and Synolakis (2004), in studying the runup distribution of both earthquake and landslide tsunamis, provided only one or two well-documented instances of landslide tsunami runup. Such poor information limits the chances of validating numerical models of landslide tsunamis against actual data. If our results will confirm that a mass failure was the main cause of the 1908 tsunami (Ryan and Heezen, 1965; Billi *et al.*, 2008), then this instance will add a useful case history to the database of landslide tsunami runup.

The 1908 Messina Earthquake and Tsunami

On 28 December 1908, at 5:21 a.m., local time, a catastrophic earthquake Mercalli–Cancani–Sieberg (MCS) maximum intensity = XI; estimated magnitude ≈ 7.1; duration ≈ 30–40 sec) struck the region of the Messina Straits between Sicily and Calabria (Fig. 1b). The earthquake caused major destruction and at least 60,000 deaths (Omori, 1909; Mercalli, 1909; Baratta, 1910). Although the causative fault of the earthquake is still poorly constrained, most models place the epicentral area in the central-southern section of the Messina Straits, off Reggio Calabria (Fig. 1b), where the maximum MCS intensities and geodetic (i.e., vertical) deformations were recorded (Loperfido, 1909; Baratta, 1910; Valensise and Pantosti, 1992; Pino *et al.*, 2000, 2009). In these models, in accordance with the local extensional regime (Neri *et al.*, 2005; Billi *et al.*, 2006) and with the leveling data acquired immediately prior and after the 1908 earthquake (Loperfido, 1909), the causative fault is assumed as normal, the coseismic slip is estimated as ranging between 1.3 and 2.7 m (Table 1), and the maximum seafloor dislocation is estimated as approximately −0.7 m (Capuano *et al.*, 1988; Valensise and Pantosti, 1992).

Within minutes of the earthquake, a tsunami with maximum measured runup of almost 12 m hit the coasts of Calabria and Sicily (Omori, 1909; Platania, 1909; Baratta,

Table 1

Estimates of Coseismic Fault Slip for the 1908 Messina Earthquake ($M \approx 7.1$) and Related References

Slip (m)*	Reference
1.5	Schick (1977)
1.5	Mulargia and Boschi (1983)
1.5	Capuano *et al.* (1988)
1.42	Boschi *et al.* (1989)
1.5	De Natale and Pingue (1991)
2.07	Pino *et al.* (2000)
1.35	Amoruso *et al.* (2002)
2.73	DISS Working Group (2007)†

*Slip estimates are mostly based on geodetic data after Loperfido (1909).

†DISS Working Group (2007) refers to a public database available online (see Data and Resources section).

1910). The cause of the 1908 tsunami has been repeatedly addressed since its occurrence; at present, the main conclusions regarding it are as follows:

1. The main evidence suggesting a nonseismic source includes the tsunami minimum travel time and maximum runup (Platania, 1909; Baratta, 1910; Billi *et al.*, 2008). These data were, in fact, recorded along the Sicilian coast near Giardini (Fig. 1b), which is approximately 40 km from Reggio Calabria, where the maximum coseismic dislocation and MCS intensities were recorded (Loperfido, 1909; Valensise and Pantosti, 1992). Based on this evidence, Omori (1909) claimed that there was a probable noncoincidence in the location of the earthquake compared with that of the tsunami.
2. In the Ionian Sea, the occurrence of a large submarine landslide connected with the 1908 earthquake is proven by the interruption of the submarine cables connecting Malta to Zakynthos, Greece, approximately 10 hours after the 1908 earthquake at a site located approximately 150 km away from the Messina Straits (Baratta, 1910; Ryan and Heezen, 1965).
3. In previous numerical simulations, the extreme runup values of the 1908 tsunami could not be explained on the basis of the seismic source alone (Tinti and Armigliato, 2003; Piatanesi *et al.*, 2008; Tappin, Watts, Grilli, Dubosq *et al.*, 2008; Favalli *et al.*, 2009).
4. In contrast with the landslide tsunami hypothesis, Gerardi *et al.* (2008), comparing the runup data for the 1908 tsunami with the expected distribution proposed by Okal and Synolakis (2004), claimed that the observed runup distribution is typical of earthquake tsunamis.

Method

Okal and Synolakis (2004) published results from numerical modeling of tsunami runup in the near-field for a dataset of 72 simulations of sources involving either earthquake dislocations or landslides. By systematically varying the parameters describing the tsunami source and the receiving beach, Okal and Synolakis (2004) quantified the influence of these parameters on the amplitude and distribution of tsunami runup. In particular, the following relationship was recognized as the function best-fitting both experimental and observed runup distributions:

$$\zeta(y) = b/\{[(y-c)/a]^2 + 1\}, \tag{1}$$

where ζ is the runup along the linear distance y that approximates the real coastline, and a, b, and c are optimized by best-fit and are, respectively, the lateral half-extent, maximum amplitude, and peak abscissa of the runup distribution. It was also empirically demonstrated that when I_1, which is the ratio between b and the coseismic slip, and I_2, which is the ratio between b and a, are greater than 1 and 10^{-4}, respectively, the main cause of the tsunami is not the seismic dislocation but a landslide. In contrast, when I_1 and I_2 are smaller than 1 and 10^{-4}, respectively, the main cause of the tsunami is presumably the seismic dislocation. A complete treatment of the relationship between runup distributions and influencing factors is available in Okal and Synolakis (2004).

To test whether the procedure that is hereafter used complies with that of Okal and Synolakis (2004), we graphically sampled the data points from six diagrams (i.e., tsunami runup versus distance diagrams) provided by Okal and Synolakis (2004), and then determined, for the six datasets (Ⓔ see Table S1 in the electronic edition of *BSSA*), the values of a, b, and c (equation 1), for which the corresponding best-fit curve minimizes the residuals between the data and the curve itself. The comparison (Table 2) between the original parameters obtained by Okal and Synolakis (2004) and those obtained in this article by the graphic sampling of data shows that the procedure used complies well with that proposed by Okal and Synolakis (2004) and that errors on I_2 connected with the graphic sampling are equal to or less than 4.3% (Table 2).

Data and Results

Through eyewitness accounts and field surveys, Platania (1909) and Baratta (1910) acquired large and accurate datasets of runup for the 1908 tsunami. These two datasets are

Table 2

Comparison between Parameters (Equation 1) Obtained by Okal and Synolakis (2004)* and the Same Parameters Obtained in This Article†

	Okal and Synolakis (2004)				This Article			
Tsunami	a (km)	b (m)	c (km)	I_2	a (km)	b (m)	c (km)	I_2 (error %)
Unimak 1946	46	31	6	6.66×10^{-4}	45.93	31.00	6.28	6.75×10^{-4} (1.3)
Mexico 1985	176	3.7	31	2.09×10^{-5}	179.79	3.69	31.16	2.05×10^{-5} (1.9)
Mexico 1995	121	4	0	3.25×10^{-5}	116.98	3.97	−0.87	3.39×10^{-5}
Nicaragua 1992	130	5.4	−7	4.15×10^{-5}	125.05	5.42	−5.85	4.33×10^{-5} (4.3)
Java 1994	219	6	22	2.75×10^{-5}	216.23	5.95	21.65	2.75×10^{-5} (~0)
Chimbote 1996	241	3.1	19	1.28×10^{-5}	246.37	3.02	−21.95	1.23×10^{-5} (3.9)

*Parameters obtained by best-fitting the runup data of six tsunamis.

†Parameters obtained by best-fitting the data obtained by the graphic sampling of dots plotted in the diagrams of Okal and Synolakis (2004). See Ⓔ Table S1 in the electronic edition of *BSSA*.

Table 3

Data (Tsunami Runup and along-Coast Distance) for Sites along the Ionian Coast of Sicily*

Site	Latitude North	Longitude East	Distance (km)†	Runup (m)	Diagram	Reference
Capo Passero	36°41'10"	15°08'18"	−136.15	1.5	Fig. 2a	Platania (1909)
Siracusa	37°04'03"	15°17'19"	−92.31	1.6	Fig. 2a	Platania (1909)
S. Panagia	37°06'25"	15°16'40"	−87.69	1	Fig. 2a	Platania (1909)
Augusta	37°13'23"	15°13'25"	−76.15	2	Fig. 2a	Platania (1909)
Brucoli	37°17'04"	15°11'17"	−70.777	4.3	Fig. 2a	Platania (1909)
Catania	37°30'03"	15°05'24"	−49.230	2.7	Fig. 2a	Platania (1909)
Ognina	37°31'23"	15°06'59"	−45.38	5	Fig. 2a	Platania (1909)
Aci Castello	37°33'21"	15°08'55"	−43.08	3.5	Fig. 2a	Platania (1909)
Aci Trezza	37°33'49"	15°09'45"	−41.54	7.1	Fig. 2a	Platania (1909)
Capo Mulini	37°34'33"	15°10'16"	−40.00	4.9	Fig. 2a	Platania (1909)
Acireale	37°36'48"	15°10'27"	−36.15	3.7	Fig. 2a	Platania (1909)
S. Tecla	37°38'10"	15°10'35"	−33.85	5.7	Fig. 2a	Platania (1909)
Stazzo	37°39'08"	15°11'42"	−32.31	4.3	Fig. 2a	Platania (1909)
Pozzillo	37°39'38"	15°11'48"	−30.77	4.8	Fig. 2a	Platania (1909)
Archirafi	37°42'40"	15°13'07"	−25.380	5.7	Fig. 2a	Platania (1909)
Riposto	37°43'56"	15°12'23"	−23.08	5.8	Fig. 2a	Platania (1909)
Fondachello	37°45'31"	15°12'53"	−20.00	5.6	Fig. 2a	Platania (1909)
Gurna	37°47'10"	15°14'05"	−16.15	5.6	Fig. 2a	Platania (1909)
Giardini	37°49'39"	15°16'09"	−10.00	9.5	Fig. 2a	Platania (1909)
Letojanni	37°52'44"	15°18'24"	−4.61	5.85	Fig. 2a	Platania (1909)
S. Alessio	37°55'29"	15°21'00"	1.54	11.7	Fig. 2a	Platania (1909)
S. Teresa	37°56'27"	15°21'50"	3.08	6	Fig. 2a	Platania (1909)
Bucalo	37°56'58"	15°22'22"	4.61	6.1	Fig. 2a	Platania (1909)
Furci	37°57'40"	15°22'55"	5.38	5.8	Fig. 2a	Platania (1909)
Roccalumera	37°58'12"	15°23'21"	6.92	8	Fig. 2a	Platania (1909)
Nizza	37°59'40"	15°24'55"	10.00	9.2	Fig. 2a	Platania (1909)
Alì	38°00'19"	15°25'32"	11.54	8.4	Fig. 2a	Platania (1909)
Itala	38°02'14"	15°27'14"	16.15	7.9	Fig. 2a	Platania (1909)
Guidomandri	38°02'31"	15°27'33"	16.92	6.4	Fig. 2a	Platania (1909)
Scaletta	38°02'52"	15°28'05"	17.69	8	Fig. 2a	Platania (1909)
Giampileri	38°03'55"	15°28'56"	18.08	7.2	Fig. 2a	Platania (1909)
Briga	38°04'39"	15°29'38"	18.46	8.5	Fig. 2a	Platania (1909)
Galati	38°06'09"	15°30'31"	20.77	8	Fig. 2a	Platania (1909)
Messina	38°11'07"	15°33'55"	33.08	3	Fig. 2a	Platania (1909)
Paradiso	38°13'37"	15°34'08"	37.69	3.7	Fig. 2a	Platania (1909)
Pace	38°14'14"	15°34'37"	38.46	4.7	Fig. 2a	Platania (1909)
Fortino	38°15'40"	15°37'57"	43.08	2.8	Fig. 2a	Platania (1909)
Torre Faro	38°15'47"	15°38'27"	43.85	0.8	Fig. 2a	Platania (1909)
Cozzo Spadaro	36°41'47"	15°07'39"	−134.62	1.5	Fig. 2b	Baratta (1910)
Calabernardo	35°52'24"	15°08'16"	−115.38	10	Fig. 2b	Baratta (1910)
Marzamemi	36°44'16"	15°07'00"	−130.00	1	Fig. 2b	Baratta (1910)
Avola	36°54'38"	15°09'03"	−112.31	1.3	Fig. 2b	Baratta (1910)
Siracusa	37°04'03"	15°17'19"	−92.31	2	Fig. 2b	Baratta (1910)
Augusta	37°13'23"	15°13'25"	−76.15	1.75	Fig. 2b	Baratta (1910)
Brucoli	37°17'04"	15°11'17"	−70.77	1.75	Fig. 2b	Baratta (1910)
Catania	37°30'03"	15°05'24"	−49.23	2.7	Fig. 2b	Baratta (1910)
Ognina	37°31'23"	15°06'59"	−45.38	5	Fig. 2b	Baratta (1910)
Aci Castello	37°33'21"	15°08'55"	−43.08	3.5	Fig. 2b	Baratta (1910)
Aci Trezza	37°33'49"	15°09'45"	−41.53	7.1	Fig. 2b	Baratta (1910)
Capo Mulini	37°34'33"	15°10'16"	−40.00	4.9	Fig. 2b	Baratta (1910)
Acireale	37°36'48"	15°10'27"	−36.15	3.7	Fig. 2b	Baratta (1910)
S. Tecla	37°38'10"	15°10'35"	−33.853	5.7	Fig. 2b	Baratta (1910)
Stazzo	37°39'08"	15°11'42"	−32.31	4.4	Fig. 2b	Baratta (1910)
Pozzillo	37°39'38"	15°11'48"	−30.77	4.8	Fig. 2b	Baratta (1910)
Archirafi	37°42'40"	15°13'07"	−25.38	5.7	Fig. 2b	Baratta (1910)
Riposto	37°43'56"	15°12'23"	−23.08	6	Fig. 2b	Baratta (1910)
Gurna	37°47'10"	15°14'05"	−16.15	5.6	Fig. 2b	Baratta (1910)
Giardini	37°49'39"	15°16'09"	−10.00	8.4	Fig. 2b	Baratta (1910)
Isolabella	37°50'33"	15°16'48"	−8.46	4	Fig. 2b	Baratta (1910)
Letojanni	37°52'44"	15°18'24"	−4.62	5	Fig. 2b	Baratta (1910)
Porto Salvo	37°55'07"	15°20'42"	0.00	6	Fig. 2b	Baratta (1910)

(*continued*)

Table 3 (*Continued*)

Site	Latitude North	Longitude East	Distance (km)†	Runup (m)	Diagram	Reference
Bucalo	37°56'58"	15°22'22"	4.62	6.1	Fig. 2b	Baratta (1910)
Furci	37°57'40"	15°22'55"	5.38	8	Fig. 2b	Baratta (1910)
Roccalumera	37°58'12"	15°23'21"	6.92	8	Fig. 2b	Baratta (1910)
Nizza	37°59'40"	15°24'55"	10.00	9.2	Fig. 2b	Baratta (1910)
Alì	38°00'19"	15°25'32"	11.54	8.4	Fig. 2b	Baratta (1910)
Itala	38°02'14"	15°27'14"	16.15	7.9	Fig. 2b	Baratta (1910)
Guidomandri	38°02'31"	15°27'33"	16.92	6.4	Fig. 2b	Baratta (1910)
Scaletta	38°02'52"	15°28'05"	17.69	8	Fig. 2b	Baratta (1910)
Giampileri	38°03'55"	15°28'56"	18.08	7.2	Fig. 2b	Baratta (1910)
Briga	38°04'39"	15°29'38"	18.46	8.5	Fig. 2b	Baratta (1910)
Galati	38°06'09"	15°30'31"	20.77	8	Fig. 2b	Baratta (1910)
Paradiso	38°13'37"	15°34'08"	37.69	3.7	Fig. 2b	Baratta (1910)
Pace	38°14'14"	15°34'37"	38.46	4.7	Fig. 2b	Baratta (1910)
Fortino	38°15'40"	15°37'57"	43.08	2.8	Fig. 2b	Baratta (1910)
Torre Faro	38°15'47"	15°38"27"	43.84	0.75	Fig. 2b	Baratta (1910)

*Data are from Platania (1909) and Baratta (1910). In each site, we reported and analyzed only the maximum runup height among those reported by Platania (1909) and Baratta (1910).

†Distances are taken along the A-A' track shown in Figure 1b.

only in part independent, as M. Baratta conducted his post-tsunami survey often comparing his measurements with those previously made by G. Platania.

We plotted the runup data acquired by Platania (1909) and Baratta (1910) on the Ionian coast of Sicily (Table 3) against distance and determined the best-fits of these data using equation (1) (Figs. 2a,b). The best-fits are characterized by a significant amplitude (b) and a narrow lateral half-extent (a), such that their ratio (I_2) is greater than 10^{-4} (Table 4). This result is consistent with the ratio I_1, which is between a minimum of 2.7 and a maximum of 6.0 depending on the coseismic slip (Table 1).

Gerardi *et al.* (2008) applied the method of Okal and Synolakis (2004) to a dataset that includes both the tsunami runup reported by Platania (1909) and Baratta (1910) and a set of runup obtained by converting the available inundation data (i.e., by Platania, 1909 and Baratta, 1910) with a relationship formulated by Hills and Mader (1997) (Fig. 2c). We graphically sampled the data points plotted by Gerardi *et al.* (2008) (Table 5), determined the best-fit of these data using equation (1), and plotted the computed best-fit in Figure 2(c). By comparing the statistical parameters associated with the best-fit curve computed by Gerardi *et al.* (2008) and with that computed in this article (Table 4), we infer that the latter one is the curve that best minimizes the residuals between the observed data and the expected distribution (see RSS, RMS, and R^2 in Table 4); hence, it is the curve that best complies with the method of Okal and Synolakis (2004). Our computed curve (Fig. 2c) is characterized by values for the parameters a, b, and c very similar

Table 4

List of Parameters for the Best-Fits (Equation 1) Shown in Figure 2

	This Article				Gerardi *et al.* (2008)
Parameter*	Figure 2a	Figure 2b†	Figure 2b'‡	Figure 2c	Figure 2c§
a (km)	41.72	52.88	46.70	50.03	110
b (m)	8.08	7.31	7.52	7.19	6.5
c (km)	−0.18	2.32	2.73	−27.39	0
c' (km)	–	–	–	~0	–
I_2	1.94×10^{-4}	1.38×10^{-4}	1.61×10^{-4}	1.44×10^{-4}	5.90×10^{-5}
RSS	82.97	145.83	66.81	120	~183
RMS	1.48	1.96	1.34	1.46	~1.81
R^2	0.65	0.40	0.70	0.64	~0.45

*c' is the value of c rectified for the difference existing between the axis origin of Figure 2c and the axis origin of Figures 2a,b. RSS is the residual sum of squares, RMS is the root mean square (i.e., the square root of the mean squared deviation of the observed data from the best-fit), and R^2 is the coefficient of determination.

†Note that RSS, RMS, and R^2 for Figure 2b are strongly influenced by the Calabernardo runup.

‡Figure 2b' designates the parameters for the best-fit of data by Baratta (1910) excluding the Calabernardo runup.

§RSS, RMS, and R^2 for the curve by Gerardi *et al.*, (2008) are designated as approximate (~) because they are computed from the graphically sampled dataset of runup (Table 5).

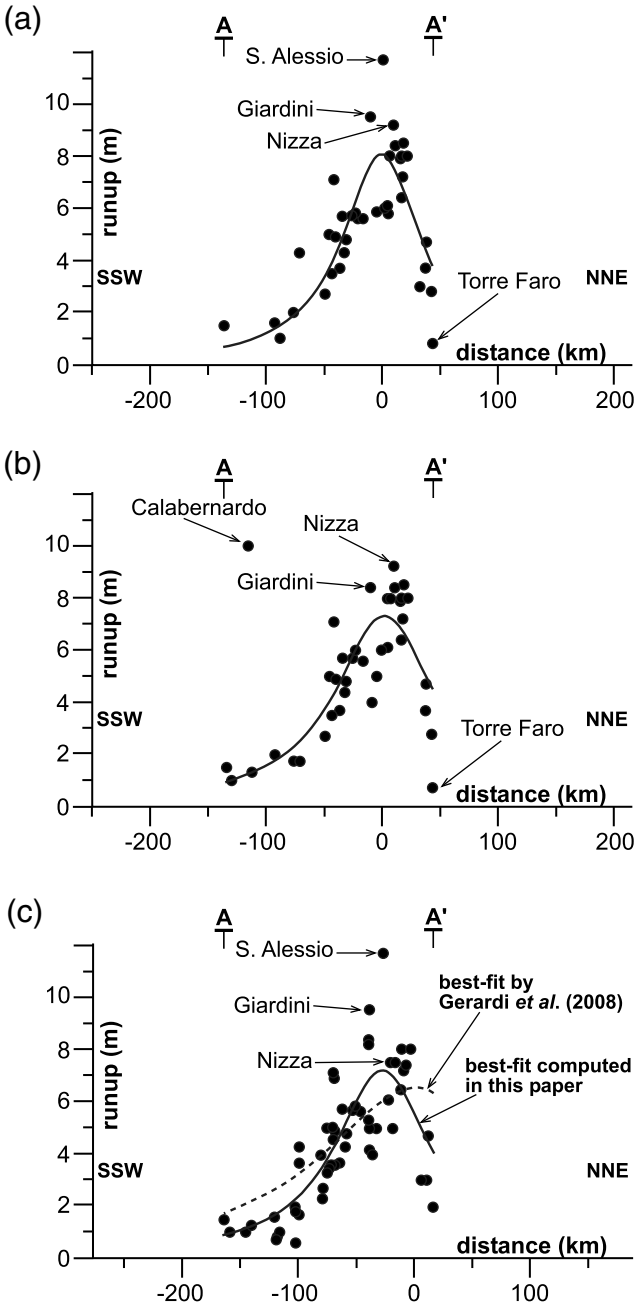

Figure 2. (a) Runup data and related best-fits (equation 1) for the 1908 Messina tsunami along the Ionian coast of Sicily. See the diagram track (A-A') in Figure 1b. Data in (a), (b), and (c) are from Platania (1909), Baratta (1910), and Gerardi *et al.* (2008), respectively (Tables 3 and 5). The best-fit parameters are reported in Table 4. (b) The best-fit involves also the runup datum from Calabernardo (i.e., 10 m), which was estimated as strongly dubious by Baratta (1910). Parameters from the best-fit of data excluding the Calabernardo runup are listed in Table 4. (c) The diagram is redrawn from Gerardi *et al.* (2008). Note that, although the three diagrams are geographically aligned (i.e., coincident), to respect the original diagram of Gerardi *et al.* (2008), the origin of axes in (c) is different from the ones in (a) and (b).

to those previously computed for the datasets of Figures 2a,b (Table 4). Moreover, the ratio I_2 is greater than 10^{-4} and is consistent with the ratio I_1, which is between a minimum of 2.6 and a maximum of 5.3 depending on the coseismic slip (Table 1).

To test the stability of the best-fit curves computed in this article (and, hence, the stability of a, b, and c) for the runup datasets of Figure 2, we ran the best-fit procedure (equation 1) on 100 subsets of each dataset (Tables 3 and 5), each subset being randomly reduced by 10% of data. We plotted the values obtained in each run for a, b, and c, and for the root mean squares, in histograms (Ⓔ see Fig. S1 in the electronic edition of *BSSA*). The results of this procedure support the stability of the computed curves.

Discussion and Conclusions

The best-fitting function (equation 1) experimentally determined by Okal and Synolakis (2004) to match the runup distribution of either earthquake or landslide tsunamis was shown to be suitable and stable also for the case of the 1908 Messina tsunami (Fig. 2 and Table 4).

The ratios I_1 and I_2 obtained from the best-fitting curves indicate that a mass failure was likely the main cause for the

Table 5

Data (Runup and along-Coast Distance) Obtained by the Graphic Sampling of Data from Figure 2c*

Runup (m)	Distance (km)	Runup (m)	Distance (km)
1.98	−16.74	5.73	62.79
2.98	−11.16	4.74	58.60
2.98	−6.98	4.19	60
4.63	−12.56	4.85	68.37
8.05	2.79	4.96	69.77
8.05	11.16	4.96	73.95
11.68	26.51	4.52	68.37
9.48	37.67	4.52	69.77
8.38	39.07	3.64	64.19
8.28	39.07	3.53	68.37
7.50	6.98	3.53	71.16
7.17	8.37	3.31	73.95
7.50	16.74	3.97	79.53
7.50	20.93	2.75	78.14
7.16	69.77	2.31	79.53
6.83	68.37	4.30	99.07
6.50	11.16	3.64	99.07
6.06	20.93	1.65	99.07
4.96	18.14	1.76	101.86
3.97	34.88	1.98	101.86
4.19	37.67	0.55	101.86
4.96	32.09	1.54	120
4.96	39.07	0.99	115.81
5.29	39.07	0.66	118.60
5.62	46.05	1.21	139.53
5.73	50.23	0.99	145.11
5.73	51.63	0.99	159.07
5.73	53.02	1.43	164.65

*Data were collected along the Ionian coast of Sicily (see A-A' track in Fig. 1b) and refer to the 1908 Messina tsunami. Figure 2c was redrawn after figure 6b of Gerardi *et al.* (2008).

1908 tsunami, thus supporting previous studies (Ryan and Heezen, 1965; Billi *et al.*, 2008; Billi *et al.*, 2009; Favalli *et al.*, 2009). The available data, however, do not allow us to exclude a contribution by the seismic dislocation on the tsunami runup (e.g., Piatanesi *et al.*, 2008; Tappin, Watts, Grilli, Dubosq *et al.*, 2008; Favalli *et al.*, 2009). According to Okal and Synolakis (2004), this contribution should not be larger than the coseismic slip, which is estimated between 1.3 and 2.7 m (Table 1). This notion is consistent with numerical simulations by Piatanesi *et al.* (2008), who obtained a maximum runup of ~2 m when considering the 1908 seismic dislocation alone, concluding that an additional landslide source is necessary to explain the observed extreme runup (~12 m).

We conclude that: (1) new geophysical and marine surveys should be accomplished in the Ionian Sea to estimate the vulnerability to mass failures and to related tsunamis; (2) in identifying and modeling the causative fault of the 1908 earthquake, the tsunami data (i.e., runup and arrival times) should be disregarded unless it is possible to quantify and separate the effects of the mass failure and seismic dislocation on both runup and arrival times of the tsunami.

The case history presented here adds to the very limited database of well-documented runup for landslide tsunamis, such a database being fundamental for validating numerical simulations of tsunamis.

Data and Resources

The DISS Working Group (2007) database was searched using www.ingv.it/DISS.

Acknowledgments

We thank C. Faccenna, R. Funiciello, and G. Neri for their encouragement; C. Poloni (http://esteco.com) for his suggestions; D. Tappin and P. Watts for insightful conversations on earthquake versus landslide tsunamis; and an anonymous reviewer for his careful review.

References

Amoruso, A., L. Crescentini, and R. Scarpa (2002). Source parameters of the 1908 Messina Straits, Italy, earthquake from geodetic and seismic data, *J. Geophys. Res.* **107,** 2080, doi 10.1029/2001JB000434.

Baratta, M. (1910). *La catastrofe sismica calabro-messinese (28 Dicembre 1908)*, Società Geografica Italiana, Roma, 426 pp. (in Italian).

Billi, A., G. Barberi, C. Faccenna, G. Neri, F. Pepe, and A. Sulli (2006). Tectonics and seismicity of the Tindari Fault System, southern Italy: Crustal deformations at the transition between ongoing contractional and extensional domains located above the edge of a subducting slab, *Tectonics* **25,** TC2006, doi 10.1029/2004TC001763.

Billi, A., R. Funiciello, L. Minelli, C. Faccenna, G. Neri, B. Orecchio, and D. Presti (2008). On the cause of the 1908 Messina tsunami, southern Italy, *Geophys. Res. Lett.* **35,** L06301, doi 10.1029/2008GL033251.

Billi, A., R. Funiciello, L. Minelli, C. Faccenna, G. Neri, B. Orecchio, and D. Presti (2009). Reply to comment by Andrea Argnani *et al.* on "On the cause of the 1908 Messina tsunami, southern Italy", *Geophys. Res. Lett.* **36,** L13308, doi 10.1029/2009GL037499.

Borrero, J. C., J. Bu, C. Saiang, B. Uslu, J. Freckman, B. Gomer, E. A. Okal, and C. E. Synolakis (2003). Field survey and preliminary modeling of the Wewak, Papua New Guinea earthquake and tsunami of September 9, 2002, *Seismol. Res. Lett.* **74,** 393–405.

Borrero, J. C., K. Sieh, M. Chlieh, and C. E. Synolakis (2006). Tsunami inundation modeling for western Sumatra, *P. Natl. Acad. Sci. USA* **103,** 19,673–19,677.

Borrero, J. C., R. Weiss, E. A. Okal, R. Hidayat, Suranto, D. Arcas, and V. V. Titov (2009). The tsunami of 2007 September 12, Bengkulu province, Sumatra, Indonesia: Post-tsunami field survey and numerical modelling, *Geophys. J. Int.* **178,** 180–194.

Boschi, E., E. Guidoboni, G. Ferrari, P. Gasperini, D. Mariotti, and G. Valensise (2000). Catalogue of strong Italian earthquakes from 461 a.C. to 1997, *Ann. Geophys–Italy* **43,** 609–868.

Boschi, E., D. Pantosti, and G. Valensise (1989). Modello di sorgente per il terremoto di Messina del 1908 ed evoluzione recente dell'area dello Stretto, in *8th Convegno del Gruppo Nazionale di Geofisica della Terra Solida*, November 1989, Rome, 245–258 (in Italian).

Capuano, P., G. De Natale, P. Gasparini, F. Pingue, and R. Scarpa (1988). A model for the 1908 Messina Straits (Italy) earthquake by inversion of levelling data, *Bull. Seismol. Soc. Am.* **78,** 1930–1947.

Davies, H. L., J. M. Davies, R. C. B. Perembo, and W. Y. Lus (2003). The Atape 1998 tsunami: Reconstructing the event from interviews and field mapping, *Pure Appl. Geophys.* **160,** 1895–1922.

De Natale, G., and F. Pingue (1991). A variable slip fault model for the 1908 Messina Straits (Italy) earthquake, by inversion of levelling data, *Geophys. J. Int.* **104,** 73–84.

Favalli, M., E. Boschi, F. Mazzarini, and M. T. Pareschi (2009). Seismic and landslide source of the 1908 Straits of Messina tsunami (Sicily, Italy), *Geophys. Res. Lett.* **36,** L16304, doi 10.1029/2009GL039135.

Fritz, H. M., W. Kongko, A. Moore, B. McAdoo, J. Goff, C. Harbitz, B. Uslu, N. Kalligeris, D. Suteja, K. Kalsum, V. Titov, A. Gusman, H. Latief, E. Santoso, S. Sujoko, D. Djulkarnaen, H. Sunendar, and C. Synolakis (2007). Extreme runup from the 17 July 2006 Java tsunami, *Geophys. Res. Lett.* **34,** L12602, doi 10.1029/2007GL029404.

Gerardi, F., M. S. Barbano, P. M. De Martini, and D. Pantosti (2008). Discrimination of tsunami sources (earthquake versus landslide) on the basis of historical data in eastern Sicily and southern Calabria, *Bull. Seismol. Soc. Am.* **98,** 2795–2805.

Hills, J. G., and C. L. Mader (1997). Tsunami produced by the impact of small asteroids, *Ann. NY Acad. Sci.* **822,** 381–394.

Ioualalen, M., J. Asavanant, N. Kaewbanjak, S. T. Grilli, J. T. Kirby, and P. Watts (2007). Modeling the 26 December 2004 Indian Ocean tsunami: Case study of impact in Thailand, *J. Geophys. Res.* **112,** C07024, doi 10.1029/2006JC003850.

Loperfido, A. (1909). Livellazione geometrica di precisione eseguita dall'I.G.M. sulla costa orientale della Sicilia, da Messina a catania, a Gesso ed a Faro Peloro e sulla costa occidentale della Calabria da Gioia Tauro a Melito di Porto Salvo, in *Relazione della Commissione Reale incaricata di designare le zone più adatte per la ricostruzione degli abitati colpiti dal terremoto del 28 dicembre 1908 o da altri precedenti*, Roma: Accademia Nazionale dei Lincei, 131–156 (in Italian).

López-Venegas, A. M., U. S. ten Brink, and E. L. Geist (2008). Submarine landslide as the source for the October 11, 1918 Mona Passage tsunami: Observations and modelling, *Mar. Geol.* **254,** 35–46.

Mercalli, G. (1909). Contributo allo studio del terremoto calabro-messinese del 28 dicembre 1908, *Atti del Reale Istituto d'Incoraggiamento di Napoli, serie 6* **7,** 249–292 (in Italian).

Mulargia, F., and E. Boschi (1983). The 1908 Messina earthquake and related seismicity, *Proc. of the International School of Physics E. Fermi*, Erice, Italy, 493–518.

Neri, G., G. Barberi, G. Oliva, and B. Orecchio (2005). Spatial variations of seismogenic stress orientations in Sicily, south Italy, *Phys. Earth Planet. Inter.* **148,** 175–191.

Okal, E. A., and C. E. Synolakis (2004). Source discriminants for near-field tsunamis, *Geophys. Int. J.* **158,** 899–912.

Okal, E. A., G. Plafker, C. E. Synolakis, and J. C. Borrero (2003). Near-field survey of the 1946 Aleutian tsunami on Unimak and Sanak Islands, *Bull. Seismol. Soc. Am.* **93,** 1226–1234.

Okal, E. A., C. E. Synolakis, B. Uslu, N. Kalligeris, and E. Voukouvalas (2009). The 1956 earthquake and tsunami in Amorgos, Greece, *Geophys. J. Int.* **178,** 1533–1554, doi 10.1111/j.1365-246X.2009.04237.x.

Omori, F. (1909). Preliminary report on the Messina-Reggio earthquake of December 28, 1908, *Bull. Imperial Earthquake Investigation Committee of Japan* **3,** 37–46.

Piatanesi, A., S. Lorito, and F. Romano (2008). Il grande maremoto del 1908: analisi e modellazione, in *Il Terremoto e il Maremoto del 28 Dicembre 1908*, G. Bertolaso, E. Boschi, E. Guidoboni, and G. Valensise (Editors), Dipartimento della Protezione Civile e Istituto Nazionale di Geofisica e Vulcanologia, Rome, 183–196 (in Italian).

Pino, N., D. Giardini, and E. Boschi (2000). The December 28, 1908, Messina Straits, southern Italy, earthquake: waveform modeling of regional seismograms, *J. Geophys. Res.* **105,** 25,473–25,492.

Pino, N., A. Piatanesi, G. Valensise, and E. Boschi (2009). The 28 December 1908 Messina Straits earthquake (M_w 7.1): A great earthquake throughout a century of seismology, *Seismol. Res. Lett.* **80,** 243–259.

Platania, G. (1909). Il maremoto dello stretto di Messina del 28 Dicembre 1908, *Bollettino della Società Sismologica Italiana* **13,** 369–458 (in Italian).

Ryan, W. B. F., and B. C. Heezen (1965). Ionian Sea submarine canyons and the 1908 Messina turbidity current, *Geol. Soc. Am. Bull.* **76,** 915–932.

Schick, R. (1977). Eine seismotektonische Bearbeitung des Erdbebens von Messina im Jahre 1908, *Geologische Jahrbuch* **11,** 3–74 (in German).

Synolakis, C. E., and U. Kânoğlu (2009). Tsunami modeling: Development of benchmarked models, in *The Sea, Tsunamis*, E. N. Bernard and A. R. Robinson (Editors), Harvard University Press, Cambridge, 237–294.

Synolakis, C. E., and L. Kong (2006). Runup measurements of the December 2004 Indian Ocean Tsunami, *Earthq. Spectra* **22,** S67–S91.

Synolakis, C. E., J. P. Bardet, J. Borrero, H. Davies, E. Okal, E. Silver, J. Sweet, and D. Tappin (2002). The slump origin of the 1998 Papua New Guinea tsunami, *Proc. R. Soc. London, Ser. A* **458,** 763–789.

Tappin, D. R., P. Watts, and S. T. Grilli (2008). The Papua New Guinea tsunami of 17 July 1998: Anatomy of a catastrophic event, *Nat. Hazard. Earth Sys.* **8,** 243–266.

Tappin, D. R., P. Watts, S. T. Grilli, S. Dubosq, A. Billi, N. Pophet, and M. P. Marani (2008). The 1908 Messina tsunami. Some comments on the source: Earthquake, submarine landslide or a combination of both?, *Eos Trans. AGU* **89,** no. (53), Fall Meet. Suppl., Abstract S41D-07.

Tinti, S., and A. Armigliato (2003). The use of scenarios to evaluate the tsunami impact in southern Italy, *Mar. Geol.* **199,** 221–243.

Valensise, L., and D. Pantosti (1992). A 125 kyr-long geological record of seismic source repeatability: The Messina Straits (Southern Italy) and the 1908 earthquake ($M_s = 7\frac{1}{2}$), *Terra Nova* **4,** 472–483.

Dipartimento di Scienze Geologiche
Università Roma Tre
Largo S.L. Murialdo, 1
Rome, 00146, Italy
billi@uniroma3.it
(A.B., L.M.)

Dipartimento di Fisica
Università della Calabria
Cosenza, Italy
(B.O.)

Dipartimento di Scienze della Terra
Università di Messina
Messina, Italy
(D.P.)

Manuscript received 30 May 2009